PROCEEDINGS OF THE INTERNATIONAL CONFERENCE NANOMATERIALS: APPLICATIONS AND PROPERTIES
Vol. **1** No 1, 01PCN38(4pp) (2012)

Characterization and Formation Mechanism of Solid Solution in Nanocrystalline Al-5wt%Si Powders Produced by Mechanical Alloying

D. Dayani[1,*], A. Shokuhfar[1], M.R. Vaezi[2], A. Zolriasatein[3]

[1] *Department of Engineering, Karaj branch, Islamic Azad University, Karaj, Iran*
[2] Division of Nanotechnology and Advanced Materials, Materials and Energy Research Center, Karaj, Iran
[3] *Advanced Materials and Nanotechnology Research Lab, Faculty of Mechanical Engineering, K.N. Toosi University of Technology, Tehran, Iran*

(Received 22 June 2012; published online30 August 2012)

Due to advantages of mechanical alloying in comparison with liquid state processes, this process has used a lot to synthesis nanostructured alloy. In the present study, aluminum and silicon elemental powders with composition Al-5wt % Si were synthesized by mechanical alloying in high energy planetary ball. X-ray diffractometer and scanning electron microscopic were used to study microstructural and morphological changes of powder particles and formation of solid solution of Al-Si during milling. Crystallite size, lattice strain and lattice parameter were determined by Scherer, Williamson–Hall and Nilson–Reley methods. Minimum crystallite size was 17.895 nm according to Scherer method and 32.644 nm according to Williamson-Hall. Solid solution of Al-Si was formed between 5 h and 30 h, due to crystallite size in nano scale and diffusion process in mechanical alloying. In addition lattice parameter changes and XRD results prove it.

Keywords: Mechanical alloying, Solid solution, Williamson-Hall, Crystallite size.

PACS number: 81.20.Ev

1. INTERODUCTION

The solid state process of materials, mechanical alloying (MA) has attracted lots of interests because of its capabilities to produce both equilibrium and non-equilibrium phases [1-4]. Mechanical alloying was developed for the first time by Benjamin [5].This technique was the result of a long search to produce a nickel-base superalloy [2]. MA is explained as a high energy milling process in which powder particles are under the influence of repeated cold welding- fracturing-welding [3]. The transfer of mechanical energy to the powder particles results in introduction of strain into the powder through generation of dislocations and other defects which act as fast diffusion paths. Additionally, refinement of particle and grain sizes occurs, and consequently the diffusion distances are reduced. It is believe that solid solution can be synthesized easily and with less energy in compare to other methods. Generally, Not only mechanical alloying is able to synthesis solid solution during milling, but it also can lead to extension of the solid solubility limits which can be estimated by X-ray diffraction (XRD), generally from changes in the lattice parameter values calculated from shifts in peak positions or even the absence of second phase peaks [2].

Aluminum alloys with low melting temperature are the most widely used material for high specific strength structural applications in various fields like transportation industry. Common way to produce Aluminum alloys is liquid state technique. According to advantages of mechanical alloying as a solid state technique in compare to liquid process which most important of them is that problems associated with melting and solidification are bypassed. So far researchers've tried to assess effect of mechanical alloying on alloying behavior of aluminum with other elements such as Cu, Mg, Zn and Pb [1, 5-9].

The present study involves mechanical alloying of Al-5wt%Si high-energy ball mill. Scanning Electron Microscope (SEM) and X-ray diffractometer (XRD) were used as characterization techniques.

2. EXPERIMENTAL PROCEDURE

A mixture of commercial aluminum (99.9% purity and particle size of 75μm) and silicon powders (99.9% purity and particle size of < 20 μm) with composition Al – 5 wt% Si was milled in a planetary ball mill under argon atmosphere. Fig. 1 shows the morphology of Al and Si powder particles. The following parameters were used ball-to-powder mass ratio of 12/1; ball diameter10 mm; speed, 250 rpm. Also 1.5wt% of stearic acid ($CH_3(CH_2)_{16}CO_2H$) was added as PCA. Mixture of powder was milled for 50hr. Samples of the milled powders were collected at different milling times:0,5, 20, 30 and 50 h.

X-ray diffraction was performed on a wide angle diffractometer in the θ-2θ step scan mode by using Cu-Kα radiation. Scans were collected over a 2θ range of 20-90° with a step of 0.01°.The crystallite size (d) and the equivalent lattice strain (ε) were determined from the broadening β) of reflections shown in Fig. 1using the Williamson-Hall method (10):

$$\beta\cos\theta = k\lambda/d + 2\varepsilon\sin\theta, \qquad (1)$$

where β is the full-width at half-maximum (FWHM) of the diffraction peak, θ is the diffraction angle, λ is the X-ray wavelength (λ_{Cu} = 0.15406 nm, d is the crystallite size and ε is the lattice strain.

Thus, it's clear cut that when we plot $\beta\cos\theta$ against $\sin\theta$ we get a straight line with slope (ε) and intercept $k\lambda/d$ The crystallite size (d) can be calculated from (K and λ are determinate) and lattice strain(ε) is slop line (11).

* dayanidavood@gmail.com

Also scherer formola was used to determine crystallite size (2):

$$d = 0.9\lambda/\beta\cos\theta, \qquad (2)$$

where β is the full-width at half-maximum (FWHM) of the diffraction peak, θ is the diffraction angle, λ is the X-ray wavelength and d is the crystallite size (2).

Furthermore the lattice parameter was obtained from a linear regression analysis of the measured lattice parameter, obtained from each peak, plotted against the Nilson–Reley function (12).

$$N - R = (\cos^2\theta/\sin\theta + \cos^2\theta/\theta)/2. \qquad (3)$$

Scanning electron microscope was used for evaluation of morphological changes.

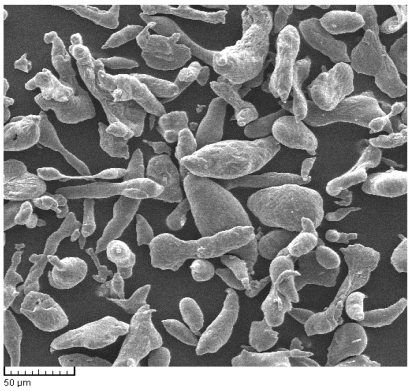

a

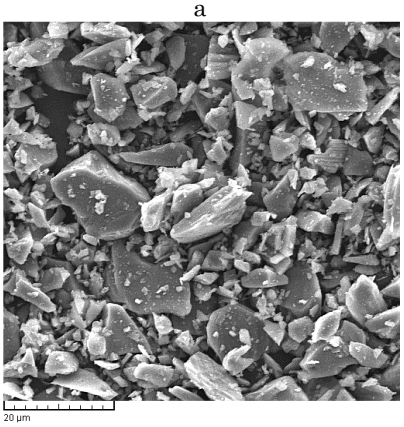

b

Fig. 1 – Secondary electron SEM micrographs of Al and Si powder particles: (a) Al and (b) Si

3. RESULTS AND DISCUSSION

Fig.2 (a) shows XRD patterns of the Al–5 wt%Si powders milled for 0,5,20,30 and 50h. In general with increasing milling time due to variation of microstructure [13], the peaks broaden which this event is shown in Fig. 1 (b).

It is well known that the crystallite size and the lattice strain contributions to line broadening are independent of each other [14].

When goal is generally to estimate trend of crystallite size change with milling time, Scherer method can be acceptable [2]. Fig. 3 (a) shows variation of crystallite size achieved by scherer formula.

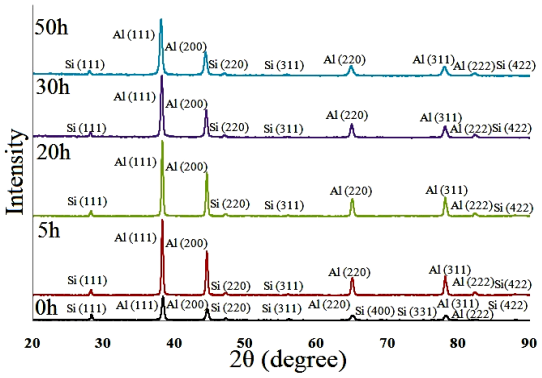

a

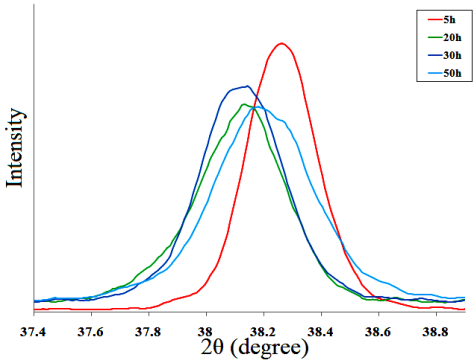

b

Fig. 2 – (a) XRD pattern of Al-5wt%Si milled for different times and (b) changes of broadening of (111) Al peak during milling

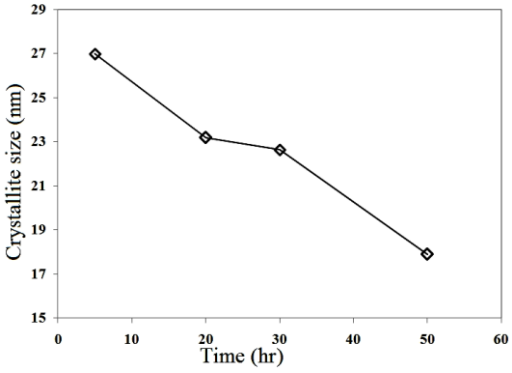

a

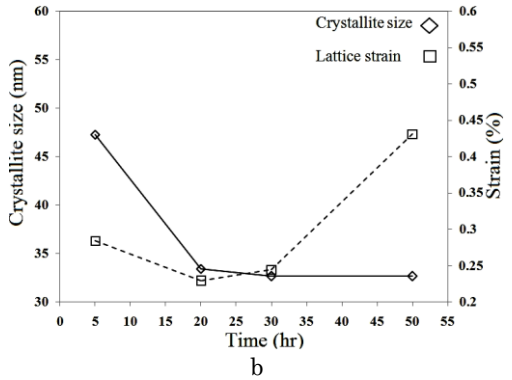

b

Fig. 3 – (a) Crystallite size as a function of milling time, determined by Scherer method and (b) shows changes of crystallite size and lattice strain which were determined from Williamson-Hall method

Also Fig. 3 (b) shows changes of crystallite size and lattice strain which were determined from Williamson-Hall method.

It is clear cut that, both Williamson-Hall and scherer methods indicate that crystallite size decreases continuously in nanometer scale. It is believed that the reason of this reduction during milling is due to the formation of new defects such as dislocations that could appear in different ways: formation of dense regions of these dislocations into the sub grains, pileup of the grain boundaries or untidy clusters within the crystallites. In general, reduction of crystallite size during milling can be contributed to dislocation generation caused by severe plastic deformation during mechanical alloying. Moreover, it is seen that lattice strain generally increases with enhancement of milling time. It is found that the increased strains can be due to stress fields associated with the multiplication of the dislocations and the introduction of dislocations, vacancies, impurities and other lattice defects during milling [11, 14].

Decrease of crystallite size can provide suitable conditions to form solid solution of Al-Si. When crystallite size decreases to a nanometer scale makes grain boundaries increase. This enhancement provide a connective network of short-circuit diffusion paths. An enhancement of self-diffusivity in comparison to boundary diffusion of a factor of about 100 has been reported. For this reason, alloying can be performance easily and by less energy [15, 16].

Furthermore, changes of lattice parameter and shifts of peaks also help to prove formation of solid solution of Al-Si. Fig. 4 and 5 show alterations of lattice parameter and the peaks shift, respectively.

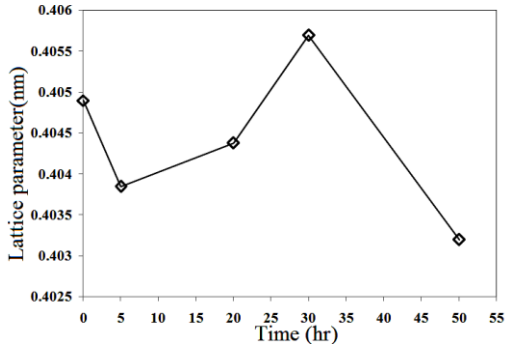

Fig. 4 – Variation of lattice parameter as a function of milling time, determined by Nilson-Reley method

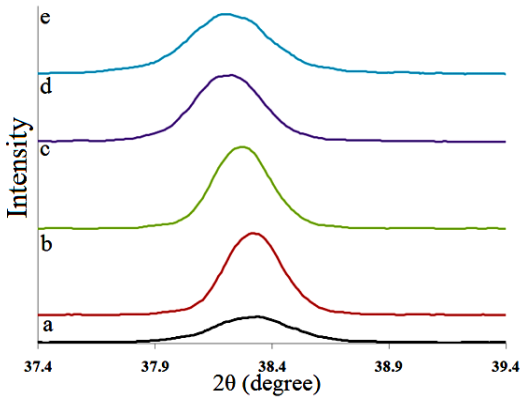

Fig. 5 – Displacement of (111) Al diffraction peak for different milling time: (a) 0 h, (b) 5 h, (c) 20 h, (d) 30 h and (e) 50 h

According to famous Bragg's law:

$$n\lambda = 2d\sin\theta, \quad (4)$$

where θ is the Bragg diffraction angle, d interplanar spacing and λ the wave length of the radiation used. In addition it is well known that there is a direct link between d and a (lattice parameter). So if lattice parameter increased which means that interplanar spacing increases, thus θ must decreases until the Bragg's law is valid [17]. It is clearly observed that after 5 h (111) Al peak moves toward higher angles while lattice parameter faces a decline. Then (111) Al peak shifts toward lower angles up to 30 h which in this duration there is an increase in lattice parameter. Afterwards lattice parameter dramatically drops to a minimum value and it makes (111) Al peak shifts toward higher angels again. Generally, it can be ascribed displacement of (111) Al peak to lattice parameter changes [18]. Also according to Vegard's law the lattice parameter of an alloy varies linearly with the solid solubility. The solid solubility increases with increasing lattice parameter of aluminum (Al = 0.4049 nm) to the lattice parameter of an diamond cubic silicon (Si = 0.543 nm) [19]. According to Fig. 4, it's seen that lattice parameter increases from 5 h to 30 h increase.

In addition it is shown in Fig. 2 (a) that two peaks of Si ((400) and (331) peaks) disappear during mechanical alloying that this issue is a next reason to prove solid solution of Al-Si was formed.

Furthermore, solid solution of Al-Si is substitutional solution which is dependence on a vacancy mechanism for diffusion and it is proved that during mechanical alloying formation of a large number of defects is unavoidable especially vacancies and because fracture of the powder particles and a lot of microcracks are generated by mechanical alloying process which these events lead to an increase in internal energy. That is why, activation energy needed for diffusion may be lowered by reducing the activation energy needed for the creation of vacancies. As a result, alloying can be performance easily [15, 16].

Fig. 6 shows SEM images of Al-5wt % Si powder particles mechanical alloyed for different milling time. In the preliminary stage of milling (5h) particles are still soft and cold welding is a predomination process. In addition, in this stage particles shape has gotten flattened because of effects of cold working during milling (Fig. 6(a)). In middle stage (20 h) particles has become more work hardening. That is why, they are fractured and fracture predominates (Fig. 6(b)). Finally, Welding and fracture mechanisms then reach equilibrium (50 h), thus particles with randomly orientated interfacial boundaries is formed and the morphology and size of particles becomes more uniform (Fig. 6(c)). As shown in Fig. 6 (c), it is obvious that after 50h the morphology of the particles is globular and the distribution of particle morphology and particle size becomes narrower.

According to Fig. 6, it is completely obvious that during milling particles size decreases. This reduction in particles size reduces the diffusion distances between particles and facilitates diffusion [11].

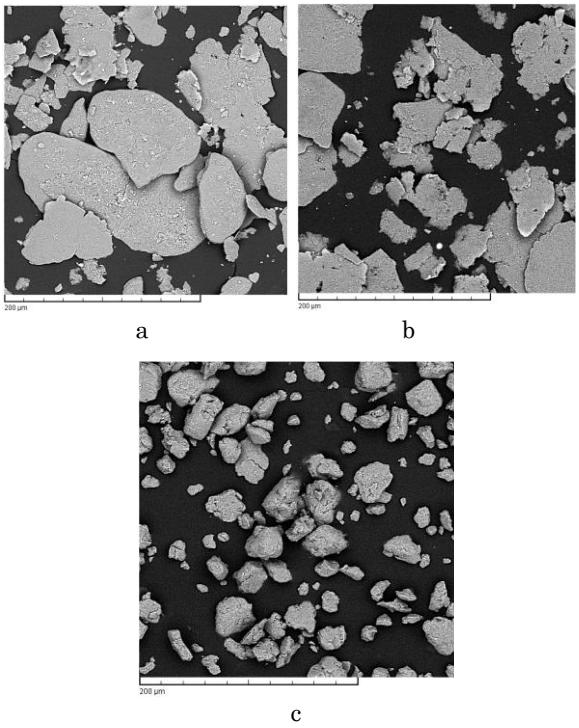

Fig. 6 – Backscatter SEM images of Al-5wt % Si powders milled for different times: (a) 5 h, (b) 20 h and (c) 50 h

The EDX analysis was performed in order to evaluate formation of solid solution. Fig. 7 shows that elemental distribution of Al and Si. It is seen that Si diffused into Al matrix, which confirms solid solution formation.

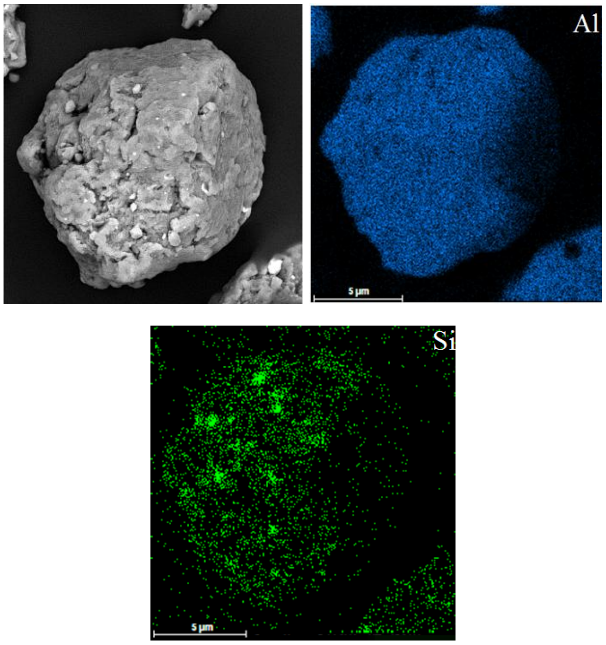

Fig. 7 – backscatter SEM image and according its elemental mapping analysis for 50 h mechanical alloyed specimen

4. CONCLUSION

In the present study, nanocrystalline Al-5wt%Si has been successfully synthesized by mechanical alloying under argon atmosphere. It was seen that after 50h the crystallite size reached to 17.895 nm according to Scherer method and 32.644 nm with strain of 0.45 % according to W-H technique. Furthermore, XRD results, SEM images and lattice parameter changes have proved solid solution of Al-Si was formed during milling. Also it has been mentioned several reason for produced solid solution of Al-Si which included formation of defects especially vacancies, reduction of crystallite size, changes of lattice parameter and decreased particle size during milling. Moreover, morphology changes of powders was evaluated. It was found that early milling welding was predominant mechanism after 20 h it was observed, fracture was major mechanism and after 50 h fracture and welding mechanisms then reached equilibrium. As a result the morphology of the particles became globular.

In addition, it was determined that formation of solid solution had been in a particular period of mechanical alloying (between 5 h and 30 h).

REFERENCES

1. S. Scudino, M. Sakaliyska, K.B. Surreddi, J. Eckert, *J. Alloy Compd.* **483**, 2 (2009).
2. C. Suryanarayana, *Prog. Mater. Sci.* **46**, 1 (2001).
3. C. Suryanarayana, *Rev. Adv. Mater. Sci.* **18**, 203 (2008).
4. E. Ma, M. Atzmon, *Mater. Chem. Phys.* **39**, 249 (1995).
5. J.B. Fogagnolo, D. Amador, E.M. Ruiz-Navas, J.M. Torralba, *Mat. Sci. Eng. A-Struc.*, **433**, 45 (2006).
6. G. Ran, J-E. Zhou, S. Xi, P. Li, *J. Alloy Compd.* **419**, 66 (2006).
7. M. Tavoosi, M.H. Enayati, F. Karimzadeh, *J. Alloy Compd.* **464**, 107(2008).
8. M. Rafiei, S. Khademzadeh, N. Parvin, *J. Alloy Compd.* **489**, 224(2010).
9. I. Manna, P. Nandi, B. Bandyopadhyay, K. Ghoshray, A. Ghoshray, *Acta Mater.* **52**, 4133 (2004).
10. G.K. Williamson, W.H. Hall, *Acta Metall. Mater.* **1**, 22 (1953).
11. J. Safari, G.H. Akbari, A. Shahbazkhan, M.D. Chermahini, *J. Alloy Compd.* **509**, 9419 (2011).
12. A. Korchef, Y. Champion, N. Njah, *J. Alloy Compd.* **427**, 176 (2007).
13. M. Mhadhbi, M. Khitouni, M. Azabou, A. Kolsi, *Mater. Charact.* **59**, 944 (2008).
14. S. Sivasankaran, K. Sivaprasad, R. Narayanasamy, P.V. Satyanarayana, *Mater. Charact.* **62**, 661 (2011).
15. L. Lu, M.O. Lai, *Mater. Design.* **16**, 33 (1995).
16. L. Lu, M.O. Lai, S. Zhang, *J. Mater. Process. Tech.* **67**, 100 (1997).
17. Z.P. Xia, J.J. Shen, Y.Q. Shen, Z.Q. Li, *J. Alloy Compd.* **448**, 210 (2008).
18. A.R. Abbasi, M. Shamanian, *j. Alloy Compd.* **508**, 152 (2010).
19. J. Milligan, R. Vintila, M. Brochu, *Mat. Sci. Eng. A-Struct.* **508**, 43 (2009).